

TURBULENCE CHARACTERIZATION BY MEANS OF WAVELETS

Maria Luiza S. Indrusiak

PROMECC – Universidade Federal do Rio Grande do Sul
Rua Sarmento Leite, 425, 90.050 - 170 Porto Alegre, Brazil
sperbindrusiak@via-rs.net

Sergio V. Möller

PROMECC – Universidade Federal do Rio Grande do Sul
Rua Sarmento Leite, 425, 90.050 - 170 Porto Alegre, Brazil
svmoller@vortex.ufrgs.br

Abstract. *This paper presents an introduction to the application of wavelets to turbulence studies. Some usual wavelets are presented and their effects on the analysis of fluctuating velocities measured in steady state and accelerating turbulent flows is discussed. A comparison with the Fourier analysis is made. Experimental results of velocity fluctuations in homogeneous turbulence and in the wake of a cylinder are obtained by means of hot wire measurements in a compact wind tunnel. Analysis of the results in steady state flow show the ability of wavelets to separate the several scales by their frequencies, being an useful tool to complement Fourier analysis. In accelerating flows, from rest to steady state, the decomposition by means of wavelets indicates the onset of turbulence and, in the flow in the wake, the growth of the shedding frequency with time.*

Key-Words: *Turbulent flow, Wavelets, Fourier analysis, hot wires*

1. Introduction

Experimental results in turbulence are usually characterized by their RMS-values, auto spectral density functions, as well as auto and cross-correlation functions, since turbulence is considered as a random phenomenon. The Fourier analysis is a valuable tool for the study of random phenomena, being widely applied to turbulence studies. Usually, random data are presented in form of discrete time series, representing a continuous (analog) function of time, sampled for digital analysis with a frequency f as a sequence of numbers at regular time intervals.

The auto spectral density function (or power spectrum) represents the rate of change of the mean square value of a certain time function $x(t)$ with the frequency w (Bendat and Piersol, 1986).

$$P_{xx}(w) = \frac{1}{BT} \int_0^T x^2(w, B, t) dt \quad (1)$$

where T is an adequate integration (observation) time and B the bandwidth.

In the Fourier space, the auto spectral density function will be defined as the Fourier transform of the autocorrelation function $R_{xx}(t)$, defined as the mean value of the product of this function at a time t , with its value at a time $t+\tau$

Let $x(t)$ and $y(t)$ be two generic functions of time, so that a correlation function of $x(t)$ and $y(t)$ can be written as

$$R_{xy}(\tau) = \frac{1}{T} \int_0^T x(t)y(t+\tau) dt \quad (2)$$

The function defined via equation (2) is called cross-correlation function. By normalizing R_{xy} by the RMS values of $x(t)$ and $y(t)$, it will be named cross-correlation coefficient function, which will be noted by C_{xy} .

The Fourier transform of equation (2) is the cross-spectral density complex function

$$P_{xy}(w) = \int_{-\infty}^{+\infty} R_{xy}(\tau) e^{-i2\pi w\tau} d\tau \quad (3)$$

The particular case of $x(t)=y(t)$ in equation (2) is called autocorrelation function R_{xx} . The Fourier transform of R_{xx} is the auto spectral density function, given by

$$P_{xx}(w) = \int_{-\infty}^{+\infty} R_{xx}(t) e^{-i2\pi w\tau} dt \quad (4)$$

The interpretation of the results of cross-spectral densities is usually very difficult, instead the coherence function is used. The coherence function is obtained by normalizing P_{xy} by the auto spectral densities of $x(t)$ and $y(t)$, thus

$$G_{xy}(w) = \frac{|P_{xy}(w)|^2}{P_{xx}(w)P_{yy}(w)} \quad (5)$$

It is well known that the turbulence study by means of Fourier analysis can give information about the frequencies involved and the interdependence of simultaneous phenomena (e. g. velocity and pressure fluctuations at different locations) (Hinze, 1975). An ergodic hypothesis of the time series is necessary for Fourier analysis of turbulence studies. In this case, mean values are independent of the sampling process. This hypothesis fails in time varying series, which means that Fourier analysis cannot deal with a signal that is changing over time and therefore its mean values are not constant. Furthermore, many processes of interest in fluid dynamics are not stationary. In accelerating flows, for instance, beside their mean values not being constant, additional phenomena may appear, as the flow velocity changes with time.

On the other side, fully developed turbulence corresponds to flows where nonlinear convection is dominant and then the Fourier representation is inadequate for describing flows in the highest limits of the Reynolds number. The convective term in Fourier space becomes a convolution, in contrast with the dissipation terms represented by the Laplace operator that becomes a diagonal in Fourier space (Farge et al., 1996).

The modern literature presents the wavelets as a tool to analyze such class of problems, including time varying series and discontinuities in this series. In the paper of Farge et al. (1996), a comprehensive review of the known applications and new possibilities of applications of wavelets to the study of turbulent flows is made. The authors show that wavelets are a promising tool to analyze such class of phenomena.

The time frequency signal decomposition through wavelet transforms was used in several different ways, like in the works of Anselmet et al. (1984) and Mouri et al. (1999), where wavelet moment analysis was performed in order to question the turbulence homogeneity at several scales, or using wavelet coefficients to make power spectrum and cross spectrum alternatively to Fourier spectra, as in the works of Hudgins et al (1993), Kishide et al. (1999) and of Perrier et al. (1995).

The purpose of this paper is to explore some classical wavelets in the study of turbulent flows by using their time frequency decomposition property to analyse the transient (accelerating) flow in a wake of a cylinder. This is a very well known flow in steady state conditions (Schlichting, 1979). For the interpretation of the results measurements in a homogeneous flow were also made.

2. Background

2.1. Spectral Analysis

Spectral analysis is essentially a modification of the Fourier analysis, more suitable for random time functions than for deterministic functions. It consists basically in the approximation of time series through a summation of sine and cosine functions called Fourier series (Chatfield, 1980).

Let $f(t)$ be a generic function, defined in the interval $[-\pi, \pi]$, which satisfies the Dirichlet conditions. Thus, $f(t)$ can be approximated by a Fourier series as

$$f(t) = \sum_w f(w) e^{iwt} \quad (6)$$

where the Fourier coefficients are the inner products of $f(t)$ with the Fourier Basis function:

$$f(w) = \frac{1}{2\pi} \int f(t) e^{-iwt} dt \quad (7)$$

A usual method (Welch, 1967) to obtain the auto spectral density function of a random time series is the approximation of blocks of smaller length of this series by a Fourier series. Figure (1) shows a schematic representation of this procedure, where a spectral window multiplies each block, so that a block begins and ends with zero. The window schematized in Fig. (1) is the Hamming window.

2.2. Wavelet Analysis

Wavelet analysis is similar to Fourier analysis in that the original function is expanded over an orthogonal basis. The Fourier basis is a set of sinusoidal functions and the wavelet basis is a set formed by dilations and translations of a single wavelet function, the so-called mother wavelet.

Ogden, 1997, describes a wavelet as a wavy function carefully constructed so as to have certain mathematical properties. An entire set of wavelets is constructed from a single “mother wavelet” so to be used to describe a large class of functions, being considered a refinement of Fourier analysis.

As the name suggests, a wavelet is a “small wave” and grows and decays essentially in a limited time period (Percival and Walden, 2000). A wavelet function tends to zero as time goes to infinity (compact support) and integrates to zero while its square integrates to unity.

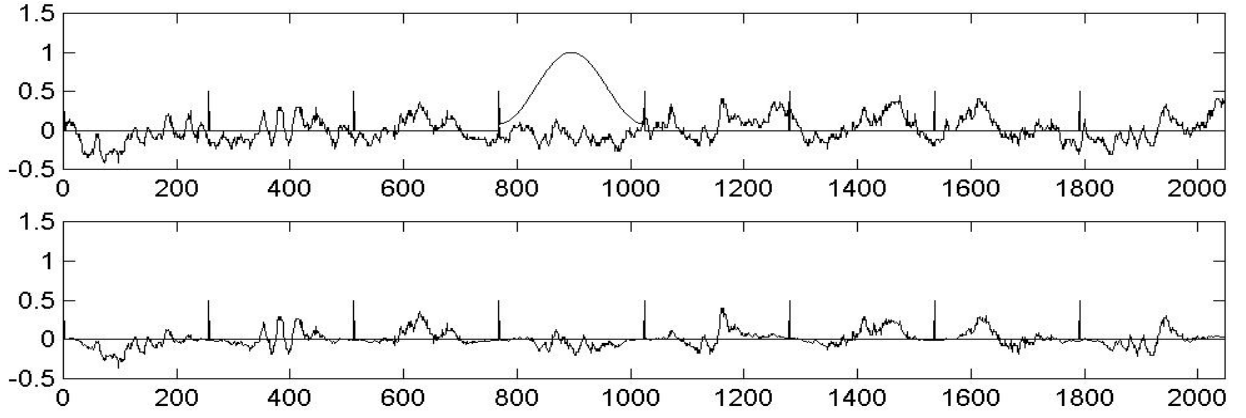


Figure 1. Schematic representation of the division of a time series in blocks multiplied by a spectral window. At first plot, the window is superimposed to the signal and the second plot is the result of the window applied to each block.

There are many different wavelets such as that developed by Yves Meyer and Ingrid Daubechies (Daubechies, 1992) and the oldest one developed by A. Haar in 1910, considered the most suitable function to the introduction and of the understanding of wavelet analysis. The Haar function is given by:

$$\Psi_{\text{Haar}}(t) = \begin{cases} 1 & 0 \leq t < 1/2 \\ -1 & 1/2 \leq t < 1 \\ 0 & \text{otherwise} \end{cases} \quad (8)$$

The simple function given by equation (8) is called a “mother wavelet”, since many others are generated through simple operations of dyadic dilations and integer translations. With j as the dilation index and k as the translation index, the wavelet family is given by

$$\Psi_{j,k}(t) = j^{-2} \Psi\left(\frac{t-k}{j}\right) \quad (9)$$

A 2^N long time series is expressed in a discrete wavelet basis as:

$$f(t) = \sum_{j=0}^N \sum_{k=1}^{2^{N-j}} d_{j,k} \Psi_{j,k}(t) \quad (10)$$

Where, as in Fourier analysis, the wavelet coefficients are simply the inner products of $f(t)$ with the corresponding basis functions:

$$d_{j,k} = \int f(t) \Psi_{j,k}(t) dt \quad (11)$$

Associated to each mother wavelet there is a father wavelet or scaling function, which also gives birth to an orthogonal basis by means of dilations and translations:

$$\Phi_{j,k}(t) = j^{-2} \Phi\left(\frac{t-k}{j}\right) \quad (12)$$

A j^{th} degree smoothed time series can be obtained combining the set $\{\Phi_{j,k}, k=1, \dots, 2^{N-j}\}$ with the scaling coefficients given by the inner products of $f(t)$ with the corresponding basis scaling functions:

$$f(t)_{j^{\text{th}} \text{ smooth}} = \sum_{k=1}^{2^{N-j}} a_{j,k} \Phi_{j,k}(t), \quad \text{where} \quad a_{j,k} = \int f(t) \Phi_{j,k}(t) dt \quad (13)$$

The decomposition of the signal with a scaling function performs an averaging of the original data over the scale interval, while wavelet transform coefficients are related differences of averages of successive scales.

The Haar scaling function is given by:

$$\phi_{\text{Haar}}(t) = \begin{cases} 1 & 0 \leq t < 1 \\ 0 & \text{otherwise} \end{cases} \quad (14)$$

Haar and other types of wavelet and scaling functions are displayed in Fig. (2). The Meyer functions are symmetric, where the two Daubechies functions are not. They are all compact supported. The wavelet functions integrate to zero and the scaling functions integrate to unity, as is easy to see for Haar functions only.

In practice, the Haar wavelet is hardly ever used because it is poorly frequency defined. The choice of the best wavelet for a given problem is not straightforward. In some situations, the results are similar for most wavelets, but for some problems, the result of the analysis depends hardly upon the wavelet type used, as will be seen later.

All the sets $\{\psi_{j,k}\}$ and $\{\phi_{j,k}\}$ are mutually orthogonal, therefore the function can be expressed as:

$$f(t) = \sum_k a_{j,k} \phi_{j,k}(t) + \sum_{j \leq J} \sum_k d_{j,k} \psi_{j,k}(t) \quad (15)$$

where a is the scale function coefficient, also called approximation coefficient, d is the wavelet function coefficient, also called detail coefficient and J is the index of the last decomposition level of interest, where the decomposition sequence, which can run until the level one, is truncated.

For a 2^N point sample, the indexes vary as below:

$$\begin{aligned} 1 &\leq j \leq J \\ 1 &\leq k \leq 2^{N-j} \end{aligned}$$

In other words, a time series $f(t)$ can be write as a sum of a coarse scaling series and J increasingly fine detail series.

Wavelet analysis can be understood as a refinement of Fourier analysis. The Fourier transform describes an original function in terms of its frequency components, over the whole domain. But for describing a signal that is changing over time, we must know the time-frequency localization of the related amplitudes. In equation (15) the coefficients $d_{j,k}$ are related to the amplitudes at a given position k , corresponding to instant $t = 2^j k \Delta t$ and a period $2^j \Delta t$, where Δt is the acquisition interval. Then, there is a vector $\{d_{j,k}\}$ associated to each frequency interval $(1/(2^{j+1} \Delta t), 1/(2^j \Delta t))$.

One-dimensional and two-dimensional wavelets are used for data and image compression as, for example, the JPEG, by applying a threshold to each set $\{d_{j,k}\}$ and $\{c_{j,k}\}$, retaining only the significant coefficients.

When used for signal processing, wavelet analysis has as a first result the detection of singularities because wavelet coefficients are very sensible to discontinuities and abrupt behavior changes of the signal.

Each set of detail coefficients retains the information concerning to a definite frequency interval and the signal can be reconstructed separately for each one of these intervals:

$$f_j(t) = \sum_{k=1}^{2^{N-j}} d_{j,k} \Psi_{j,k}(t) \quad (16)$$

These sets $f_j(t)$, which are part of the original signal, point out the localized time behavior of the signal at the corresponding frequency interval. However, the width of the frequency interval depends on the decomposition level, being larger for higher frequencies.

To obtain narrower frequency intervals another wavelet decomposition procedure must be used. Regarding each detail coefficient vector as a series by itself and decomposing that series using the same wavelet and scaling functions, two series with respectively lower and upper half width frequency interval are obtained. This scheme, applied recursively at all levels, generates a “wavelet tree”, shown in Fig. (3) for $j=3$ and is called wavelet packet transform. Each wavelet packet transform is associated with a level j , and the j^{th} level decomposes the frequency interval of the original signal $[0, f/2]$ into 2^j equal and individual intervals (Percival and Walden, 2000).

The first advantage of this band pass filter action of wavelet packet decomposition is that, by reconstructing separately each frequency interval, according to Eq. (16), the signal can be seen and its behaviour analysed in a time frequency domain.

3. Experimental Technique

The test section is a 1370 mm long rectangular channel, with 146 mm height and a maximal (adjustable) width of 193 mm, Fig. (4). Air, at room temperature, is the working fluid, driven by a centrifugal blower, passed by a diffuser and a set of honeycombs and screens, before reaching measurement location with about 2 % turbulence intensity.

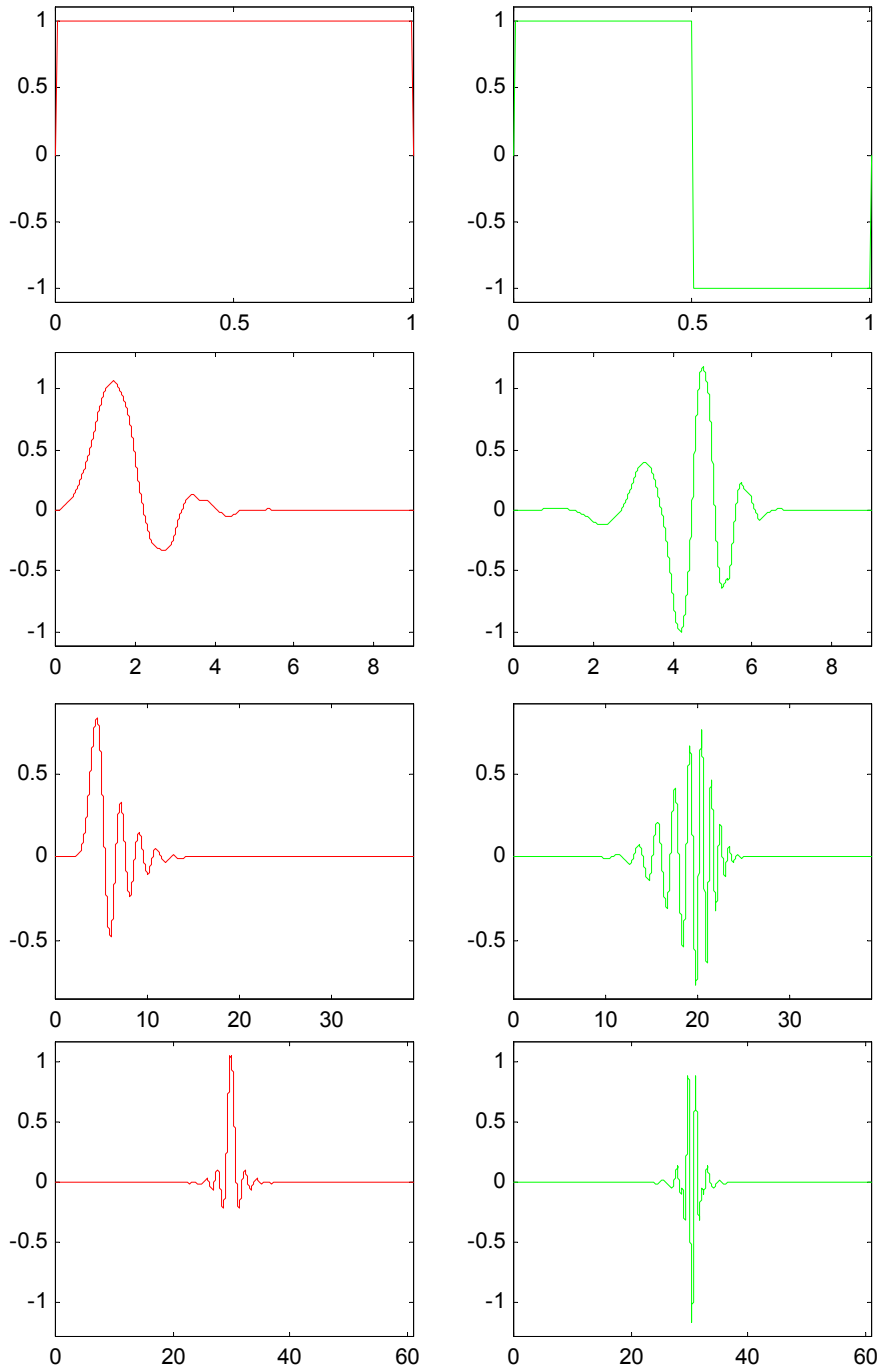


Figure 2. Some scaling and wavelet functions: from above, Haar, Daubechies 5, Daubechies 20, Meyer

For measurements of velocity and velocity fluctuations, DANTEC constant temperature hot wire anemometers were applied. A single and a double hot wire probes were applied. The double wire probe; has one wire perpendicular to the main flow and a second wire inclined 45° to the main flow, so that two components of the velocity vector and their fluctuations could be measured simultaneously.

Data acquisition of velocity fluctuations was performed with a Keithley DAS-58 A/D-converter board with a sampling frequency of 25 kHz, and a low pass filter set at 10 kHz.

Two time series, shown in Fig. (5), were acquired in a transient flow, starting from rest and running to the stationary state. The first series was acquired with a single tube assembled perpendicular to the flow, in order to produce a vortex street and the other was acquired, for comparison, in the wind tunnel free flow, which was considered homogeneous at the measurement location.

Wavelet analysis was performed using the Matlab 5.3 software.

Analysis of uncertainties in the results has a contribution of 1.4 % from the measurement equipments (including hot wire and A/D converter). The mean error of the determination of the flow velocity with a hot wire is about 3.4%. Velocity fluctuations in the main flow direction are obtained with a mean error of 15%, while transverse velocity has an error of about 30%.

4. Results

Figure (5) shows the transient signals acquired in the wind tunnel. These and the subsequent plots were performed using sampling points instead of time. The last point of the series (2^{18}) corresponds to 10.4857 seconds.

The power spectrum of the last half part of the vortex street series, Fig. (6), where steady state is reached, shows 103.7 Hz as the predominant frequency of vortex shedding in the wake. This is in agreement with the frequency of 98.5 Hz obtained by using the Strouhal number of 0.21.

The choice of the wavelet function in the wide wavelet world was made following a best filtering criterion. A previous selection the classical Haar wavelet, a symmetric wavelet (Meyer) and two asymmetric wavelets (Daubechies 5 and Daubechies 20) were used to decompose the steady part of the original signal to the 11th level, corresponding to frequency bands of 6.1 Hz.

Figure (7) shows the power spectra of the 11th level reconstructed approximation and the first two reconstructed detail time series (only one for Haar) and the plotting of the reconstructed approximation time series for each wavelet functions.

The reconstructed detail and approximation series with Daubechies 20 functions have significant spectral densities only at expected frequency interval, while reconstructed series with Meyer functions show significant spectral densities out the expected frequency interval. This occurs mainly for the reconstructed approximation whose expected frequencies rise up to 6.1 Hz. Therefore the reconstructed approximation, shown at right of Fig. (7), is not a smoothed version of original signal.

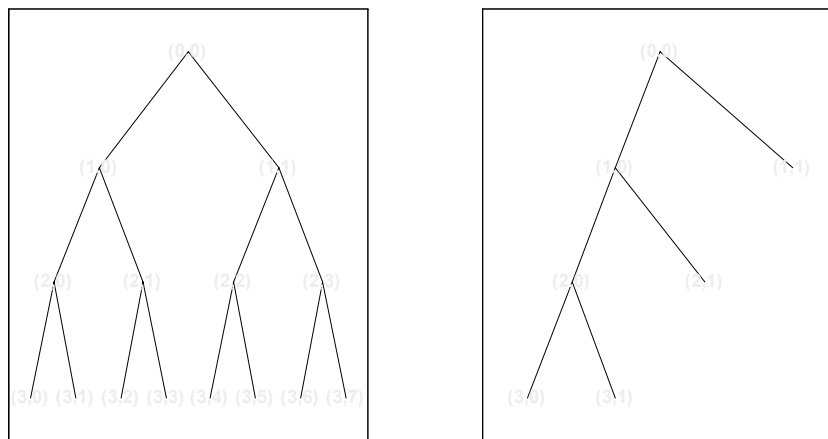


Figure 3. Wavelet tree for $j=3$, using wavelet packet transform and at right, a same level wavelet tree for simple wavelet transform.

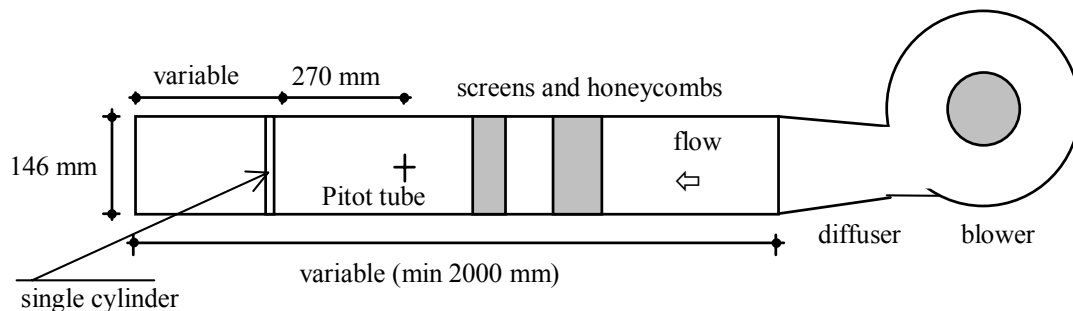


Figure 4: Schematic view of the test section

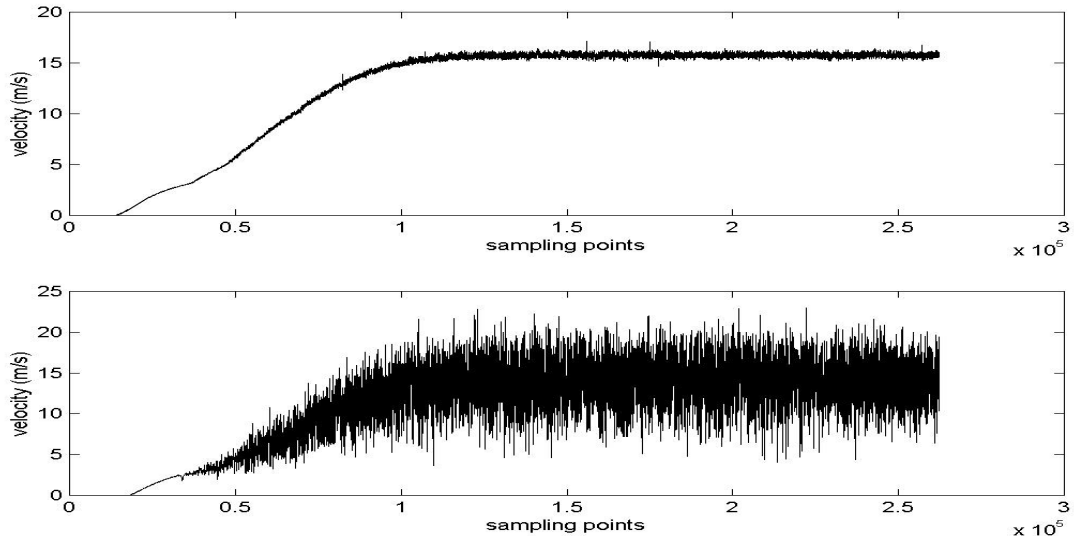


Figure 5. Time series obtained at free wind tunnel and with a transverse tube causing a vortex street.

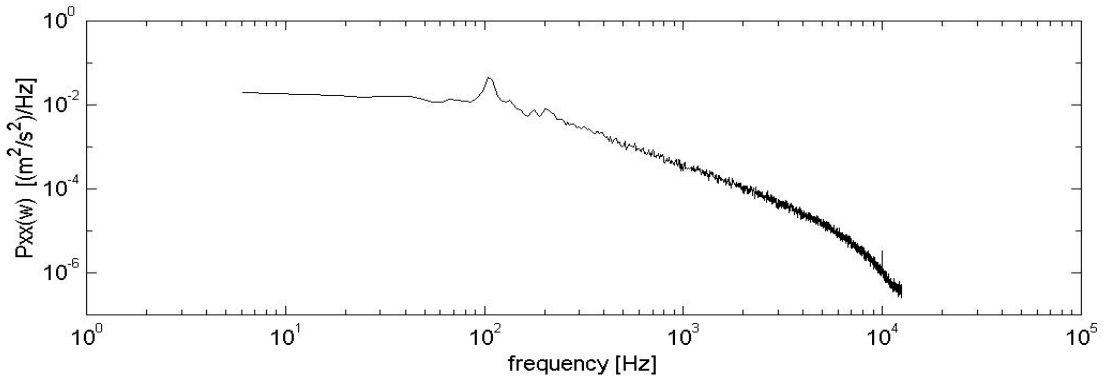


Figure 6. Power spectrum of last half part of the second signal showed in Fig. (4)

The power spectra of reconstructed approximation and first detail series concerning Haar functions show that they are not well frequency localized. It is noticeable that all but Haar transforms show end effects that should be removed for some further analysis, like moment analysis.

The power spectra relating to Daubechies 5 functions show less separation between frequency bands than for Daubechies 20 spectra.

According to the above explained, Daubechies 20 was chosen as the most suitable wavelet function for the proposed study.

To analyze the vortex street development, the transversal velocity fluctuation, perpendicular to both tube and tunnel axis, was computed from the signals obtained by the double wire probe. An 11th level wavelet packet decomposition was applied to the time series and then the 11th level nodes were reconstructed according to Eq. (16). The results for the nodes concerning frequencies up to 128 Hz were displayed in Fig. (8).

Departing from 30.5 Hz, each signal of Fig. (8) left shows clearly a transient increase of amplitudes which occurs later for higher frequencies, up to 103,7 Hz, showing the presence of the vortex shedding at the corresponding frequency and time. At next frequency interval, 103.7 to 109.8 Hz, the amplitude increase, which begins nearly the onset of stationary velocity, holds until the end of the time series. At frequencies above 109.8 Hz, the sequence of transient increased amplitudes disappears and there is only a slight difference in the amplitudes at the part of the signal that corresponds to the steady state. For frequencies lower than 30.5 Hz, the presence of the amplitudes of the vortex shedding is not very clear and may be confused with the onset of the turbulence.

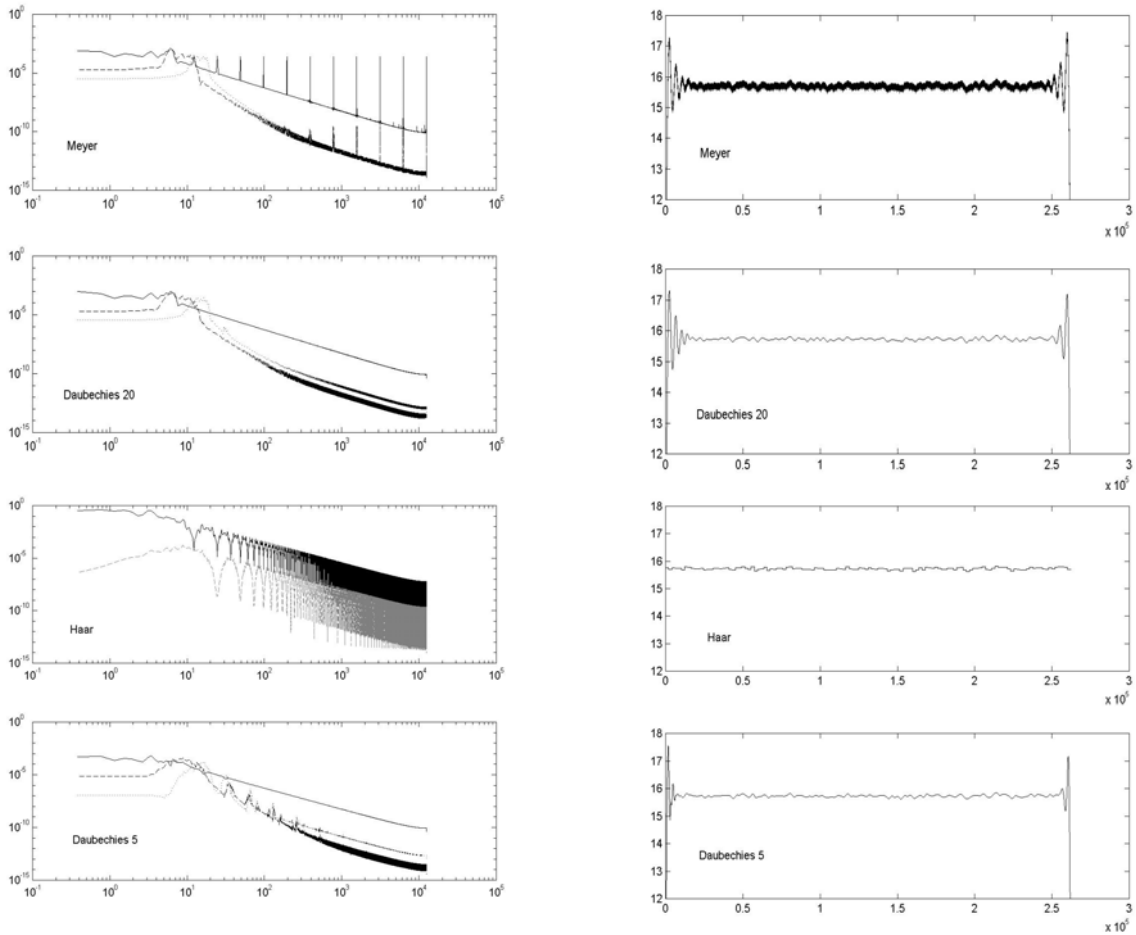


Figure 7. PSD plots and reconstructed approximation time series of the same signal, namely a stationary wind tunnel longitudinal velocity record. The decompositions were performed to the 11th level using a wavelet packet scheme, with Meyer, Daubechies 20, Haar and Daubechies 5 functions. Each reconstructed signal corresponds to a frequency interval of 6.1 Hz.

The transverse velocity fluctuation of the free wind tunnel transient, band-pass filtered with the same wavelet packet scheme and displayed in Fig. (8) right, suggests only that all frequency bands are present from just after the beginning of the movement (see Fig. (5)) and that the amplitudes, which are related to the distribution of the energy at each frequency band are a bit inhomogeneous along the time and about twenty times lower than at vortex street series.

At the vortex street, all the frequencies are more energized and the predominant frequency of the wake is the frequency of the energy carrying eddies. In Fig. (8) left one can see, at almost all frequency bands, that the amplitudes are lower before the point that denotes the wake frequency than after that point. This seems to be due to the fact that only after their birth the energy carrying eddies can transfer energy to the smaller eddies, thus after the point denoting the presence of the wake at a certain band frequency, the subsequent (higher) frequency bands show higher energy levels than previously.

In order to relate the transient vortex shedding frequencies and the free stream transient velocities approaching the cylinder, another experiment was performed. At same transient conditions, two single wire probes were mounted at free stream, one before the tube and another in the wake of the cylinder. The transient approaching free stream velocity, U_{app} , and the transient longitudinal velocity in the wake of the cylinder, U , were simultaneously acquired.

A 13th level smoothed version of U_{app} was obtained according to Eq. (13), using Daubechies 20 scaling function. The transient wake velocity series, U , was band filtered with Daubechies 20 wavelet packet, as was already done with the transverse component. The progress of the wake frequency is less evident at longitudinal than at transversal component of velocity, but is also visible. For each frequency band, the mean point of transient increase of amplitudes, which denotes the time frequency location of transient wake, was used to find the corresponding incident transient velocity, according to the scheme shown at Fig. (9). Some uncertainty in the determination of such points is due to the vortex shedding process, which does not occur at a single distinct frequency, but rather it wanders over a narrow band of frequencies with a range of amplitudes (Blevins, 1990).

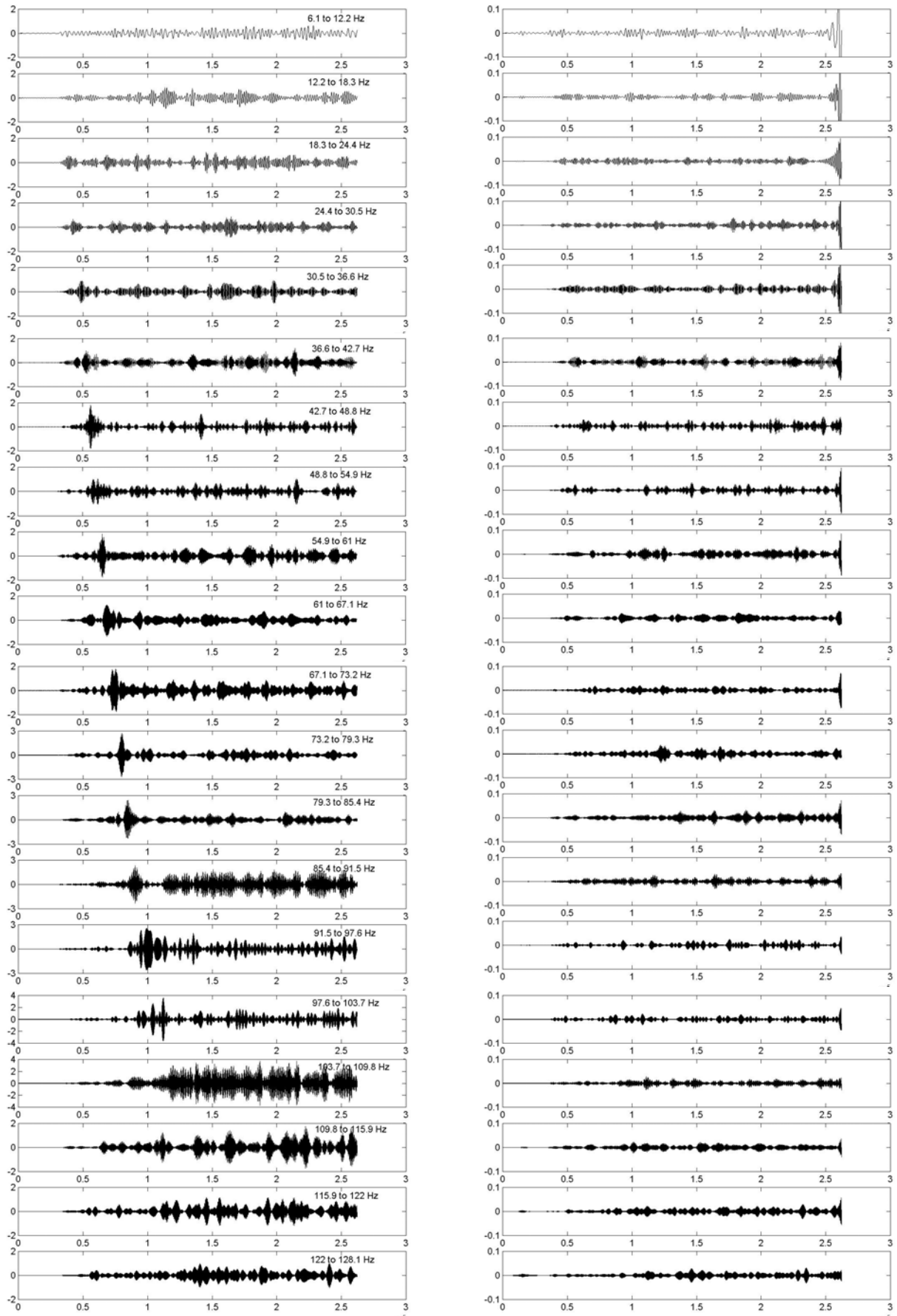


Figure 8. Reconstructed detail series up to 128 Hz, using a 11th level wavelet packet decomposition with Daubechies 20 functions. At right, the time series is the transverse component of the transient time series acquired with the single tube vortex street and, at left, the transverse component of the free wind tunnel transient velocity.

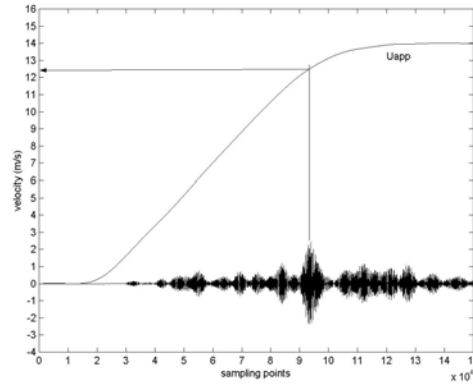


Figure 9. Time location of the transient vortex shedding and respective transient free stream velocity, for the frequency band 79.3 to 85.4 Hz.

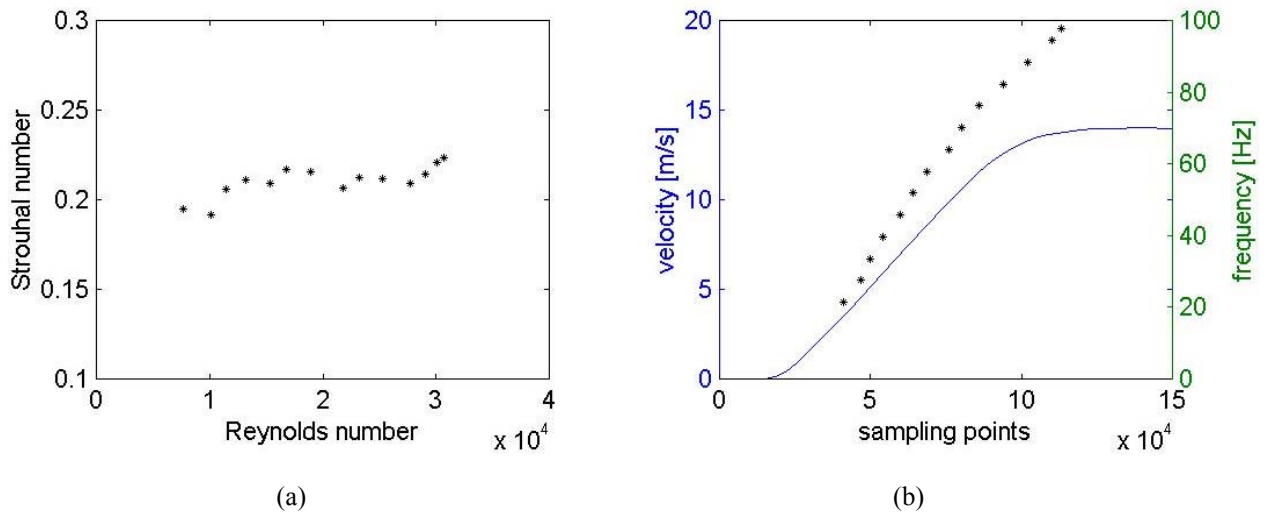


Figure 10. a- Strouhal numbers $Str(t)$ computed from transient frequency and approaching velocity against Reynolds number based on tube diameter. b- transient frequency and approaching velocity.

The transient Strouhal number can be evaluated as:

$$Str(t) = \frac{\overline{w_s}(t) D}{\overline{U}_{app}(t)} \quad (16)$$

where D is the tube diameter, \overline{U}_{app} is the instantaneous mean approaching velocity and $\overline{w_s}$ is the mean frequency of the band.

Figure (10-a) shows the values the transient Strouhal numbers $Str(t)$ computed from transient frequency and approaching velocity against Reynolds number based on tube diameter, together with the transient vortex shedding $\overline{w_s}(t)$, obtained for each band and the transient velocity, Fig (10-b), plotted against the corresponding sampling points. Like the transient velocity, the vortex shedding frequency has almost a linear time variation and, therefore, the transient Strouhal number is considered constant along time. The variations observed are due to the experimental inherent uncertainties and the frequency resolution of the wavelet analysis.

5. Concluding Remarks

In this article the well known vortex street due to a stationary cylinder perpendicular to a turbulent flow was studied in a multiresolution analysis context, with the transient regime being analyzed using the wavelet tools.

The property of band pass filter provided by the concurrent use of wavelet and scaling functions, in a so-called wavelet packet transform, enabled the capture of the behavior of the wake in an accelerating flow. The energy distribution could be observed at each frequency band, which can be done as narrow as desired.

The smoothing property of wavelet decomposition and reconstruction of lower frequencies of the original transient signal is also very useful to obtain an instantaneous mean, as was done in this research work, and in extracting that mean from the signal to obtain the fluctuation.

The good agreement of the transient Strouhal number computed from parameters obtained in wavelet analysis with the classical stationary Strouhal number of 0.21, corroborates the proper use of wavelet for the transient turbulent wake analysis.

6. List of Symbols

a	Wavelet approximation coefficient.
B	Bandwidth.
C_{xx}	Auto correlation coefficient function.
C_{xy}	Cross correlation coefficient function.
d	Wavelet detail coefficient.
D	Diameter - m.
f	Generic function.
G_{xy}	Coherence function.
j	Index.
k	Index.
P_{xx}	Auto spectral density function - $(m^2/s^2)/Hz$.
P_{xy}	Cross spectral density function - $(m^2/s^2)/Hz$.
Re	Reynolds number $(U.D/\nu)$.
R_{xx}	Auto correlation function.
R_{xy}	Cross correlation function.
Str	Strouhal number $(w.D/U)$.
t	Time - s.
T	Total sampling time - s.
U	Velocity – m/s.
x	Generic function.
y	Generic function.
w	Frequency – Hz.
ν	Kinematic viscosity – m^2/s .
ϕ	Generic scale function.
Ψ	Generic wavelet function.
τ	Time interval – s.

7. References

- Anselmet, F., Gagne Y., Hopfinger, E. J., 1984, High-order velocity structure functions in turbulent shear flows, *J. Fluid Mech.*, vol, 140, pp.63-89
- Bendat, J. S. and Piersol, A. G., 1990. *Random Data – Analysis and Measurement Procedures*, 2nd Ed., New York: Wiley.
- Blevins, R. D., 1990, *Flow-Induced Vibration*, 2nd Ed., Van Nostrand Reinhold, New York
- Chatfield, C., 1980. *The Analysis of Time Series – An Introduction*, New York: Chapman and Hall.
- Farge, M., Kevlahan, N., Perrier, V. and Goirant, E., 1996. Wavelets and Turbulence, *Proceedings of the IEEE*, Vol. 84, pp. 639-669.
- Hinze, J. O., 1975. *Turbulence*, New York: Mc Graw-Hill.
- Hudgins, L., Friehe, C. A. and Mayer, M. E., 1993, Wavelet Transforms and Atmospheric Turbulence, *Physical Review Letters*, vol. 71, n. 20, pp. 3279-3282
- Kishida, K., Araki, K., Kishiba, S. and Suzuki, K., 1999, Local or Nonlocal? Orthonormal Divergence-Free Wavelet Analysis of Nonlinear Interactions in Turbulence, *Physical Review Letters*, vol. 83, n. 26, pp. 5487-5490.
- Mouri, H., Kubotani, H., Fujitani, T., Niino, H. and Takaoka, M., 1999, Wavelet analyses of velocities in laboratory isotropic turbulence, *J. Fluid Mech.*, vol. 389, pp. 229-254.
- Ogden, R. T., 1997. *Essential Wavelets for Statistical Applications and Data Analysis*, Boston: Birkhäuser.
- Percival, D. B. and Walden, A. T., 2000, *Wavelet Methods for Time Series Analysis*, Cambridge University Press
- Perrier, V., Philipovitch, T. and Basdevant, C., 1995, Wavelet Spectra compared to Fourier Spectra, *J. Math. Phys.*, 36, pp. 1506-1519
- Schlichting, H., 1979. *Boundary-Layer Theory*, New York: McGraw-Hill.
- Welch, P. D., 1967. The use of Fast Fourier Transform for the estimation of power spectra: a method based on time averaging over short, modified periodograms, *IEEE Trans. Audio and Electroacoustics*, AU-15, pp. 70-73.